Droplet epitaxy quantum dots based infrared photodetectors

(Article begins on next page)

09 April 2024

Droplet epitaxy quantum dots based infrared photodetectors

Stefano Vichi,[1] Sergio Bietti,[1] Arastoo khalili,[2] Matteo Costanzo,[1] Federica Cappelluti,[2] Luca Esposito,[1] Claudio Somaschini,[3] Alexey Fedorov,[4] Shiro Tsukamoto,[1] Patrick Rauter,[5] and Stefano Sanguinetti[1]

[1] *LNESS and Department of Materials Science, University of Milano-Bicocca, via Cozzi 55, 20125 Milano, Italy*

[2] *Department of Electronics and Telecommunications, Politecnico di Torino, Corso Castelfidardo 39, 10129 Torino, Italy*

[3] *PoliFab - Politecnico di Milano, via Colombo 81, 20133 Milano, Italy*

[4] *CNR–IFN and LNESS, via Anzani 42, 22100 Como, Italy*

[5] *Institute of Semiconductor and Solid State Physics, Johannes Kepler University of Linz, Altenberger Strae 69, 4040 Linz, Austria*

I. ABSTRACT

The study, fabrication and characterization of an infrared photodetector based on GaAs droplet epitaxy quantum dots embedded in $Al_{0.3}Ga_{0.7}As$ barrier is reported. The high control over dot electronic properties and the high achievable number density allowed by droplet technique permitted us to realize a device using a single dot layer in the active region. Moreover, thanks to the independent control over dot height and width, we were able to obtain a very sharp absorption peak in the thermal infrared region (3-8 μm). Low temperature photocurrent spectrum was measured by Fourier spectroscopy, showing a narrow peak at 198 meV (~ 6.3 μm) with a full width at half maximum of 23 meV. The observed absorption is in agreement with theoretical prediction based on effective mass approximation of the dot electronic transition.

II. INTRODUCTION

In recent years the market of infrared (IR) devices is continuously growing, pushed by the great number of applications in commercial, public, military and academic domains. However, the further development of IR sensors for imaging purposes is closely linked to the development of a new generation of sensor: the "third generation"[1].

This new generation should provide photodetectors with enhanced capabilities such as larger number of pixels, higher frame rates, better thermal resolution and multispectral functionality. In the IR region four major photodetector technologies are developing multispectral capabilities: the HgCdTe photodiodes, the quantum well (QWIP) and quantum dot (QDIP) infrared photodetectors and antimonide based type II superlattice photodiodes[2]. The last three technologies are based on quantum heterostructures, making them suitable for easy integration in present technology. Monolithic silicon integration of both As and Sb materials, at the basis of the three technologies, have been already demonstrated[3–5]. Between these, bulk HgCdTe is at present times the most advanced technology, with better overall performances and a wide and tunable detection window[6]. However, QDIP photodetectors are emerging as a promising technology, due to the high control over transition energies originating from 3D carrier confinement and the absence of limiting selection rules, which hinder the widespread use of QWIP technology[6,7]. The active part of these detectors consists

2

of multiple layers of self-assembled quantum dots (QDs) embedded in a barrier layer with a larger band gap for carrier confinement in three dimensions. QDs are usually self-assembled via the Stranski-Krastanov (SK) growth mode, which exploits the strain induced by lattice mismatch between substrate and epilayer to assemble the nanostructures[8,9]. However, there are several drawbacks which need to be overcome before SK-QD based QDIPs may become the leading technology in the thermal infrared (TIR) range. The main disadvantage of SK-QDIPs is related to the large size dispersion which broadens the absorption spectrum and subsequently lowers quantum efficiency[10]. The other drawbacks, related to the growth process, are the presence of strain-related defects and of a wetting layer which lowers the carrier confining barrier. Most of these shortcomings can be overcome by using droplet epitaxy (DE), an alternative technique to grow self-assembled QDs in lattice-matched materials. The much higher control over the dot nucleation process allows to tune independently QD geometry, width, thickness and density and to achieve a lower size dispersion[11], which leads to a higher absorption coefficient and a narrower bandwidth. These advantages make DE a very interesting technique to grow quantum dots, in particular for photodetectors where high absorption coefficient and narrow bandwidth are required. In this paper we present the first example of working QDIP for TIR detection based on $GaAs/Al_{0.3}Ga_{0.7}As$ DE-QDs.

III. EXPERIMENTAL PROCEDURE

The growth was performed in an MBE system, starting from an intrinsic double polished 2" GaAs-(001) substrate. The structure consists of an active region sandwiched between two contact layers. The bottom contact consists of a first layer of 1.5 μm Si-doped GaAs layer with a nominal doping of $2 \cdot 10^{18}$ cm^{-3}, followed by 100 nm of Si-doped $Al_{0.3}Ga_{0.7}As$ with a nominal doping of $3 \cdot 10^{17}$ cm^{-3}. The active region is made of 700 nm thick intrinsic $Al_{0.3}Ga_{0.7}As$ layer in which, at the center, a single GaAs QDs layer is embedded. The QDs, grown by droplet epitaxy, are filled by an underlying δ-doping layer positioned 3 nm apart from the QDs, providing nominally 6 electrons per dot. QD growth conditions were optimized to obtain the desired size and density by growing a series of uncapped samples and characterizing them by AFM, performed in tapping mode and using a tip with a lateral resolution of 2 nm. Following the intrinsic region, 100 nm of Si-doped $Al_{0.3}Ga_{0.7}As$ with a doping of $3 \cdot 10^{17}$ cm^{-3} were grown. Finally, 1 μm of n doped GaAs with a doping density

3

of $2 \cdot 10^{18}$ cm^{-3} was deposited as a top contact.

More in details, the growth rate was kept at 0.5 ML/s for the GaAs and 0.71 ML/s for the AlGaAs layers, the substrate temperature was set to 580°C and 650°C for GaAs and AlGaAs, respectively. QDs were grown by depositing 3ML of Ga at a rate of 0.1 ML/s with a substrate temperature of 180°C. At the same temperature the crystallization was performed by supplying As at a beam equivalent pressure of $5 \cdot 10^{-5}$ Torr. After the growth, standard photolithography was used for structuring the device. Mesa etching was done by a wet approach, using an H$_3$PO$_4$:H$_2$O$_2$:H$_2$O solution with 1:2.5:8 relative concentrations. Metal contacts were finally deposited by e-beam evaporation using a stack of Ge(26 nm)/Au(54 nm)/Ni(15 nm) and annealed at 420°C for 5 s in Ar forming gas, in order to get ohmic contacts as confirmed by I-V measurements. The device structure is shown in figure 1.

For optoelectronic characterization at cryogenic temperatures, the devices were contacted by wire bonding and mounted in a cryostat.
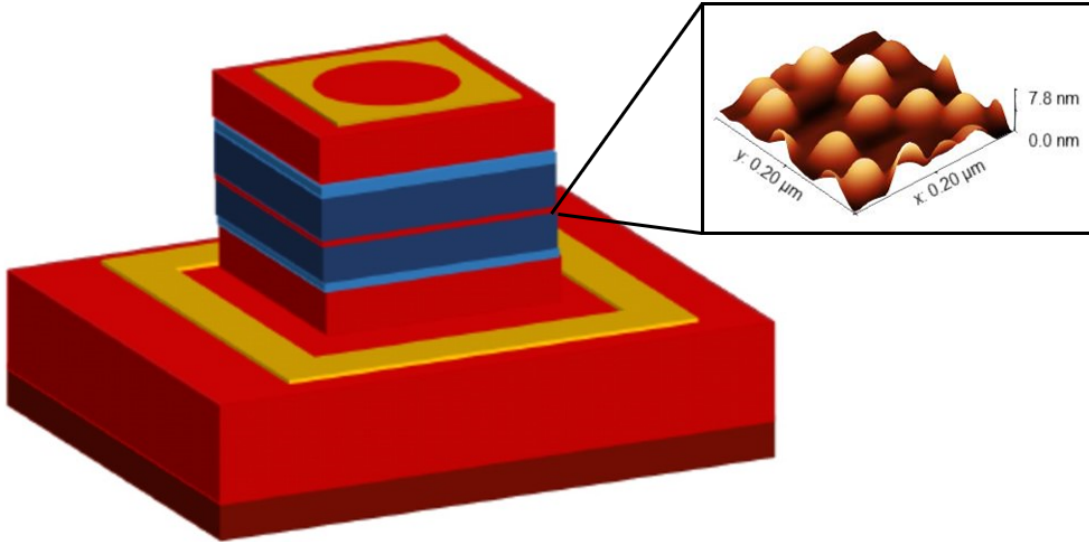

FIG. 1: Design of the device, where different materials are represented by different colors: gold for the contacts, red for GaAs, light blue for doped Al$_{0.3}$Ga$_{0.7}$As and blue for intrinsic Al$_{0.3}$Ga$_{0.7}$As. The size of the mesa is 1x1 μm. The inset shows a 200x200 nm AFM scan of the QDs.

IV. RESULTS AND DISCUSSION

The quantum dot geometry was studied by atomic force microscopy (AFM) on an un-capped samples. As can be seen from figure 2b, the shape of the dots shows a slight asymmetry due to the diffusion coefficient of Ga adatoms being larger along $<1\bar{1}0>$ compared to $<110>$ direction[12]. We defined the width of the dots as the diameter of the circle which gives the same projected area as the dot. Accordingly, from the analysis of the AFM images (figure 2a) we calculated a dot density of $3.8 \cdot 10^{10}$ cm^{-2} with a mean height of $5.1 \pm 1nm$ and a diameter of $36 \pm 8nm$.

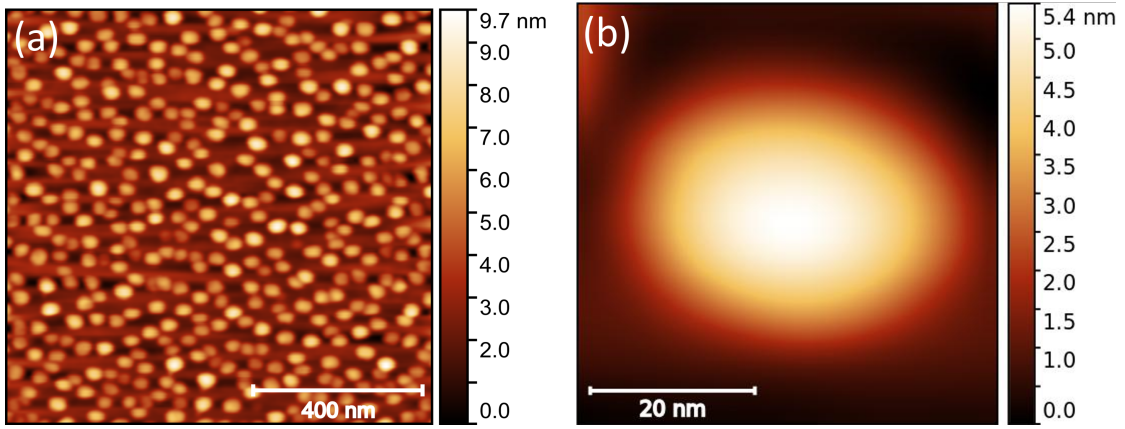

FIG. 2: (a) AFM image of the dot population of the uncapped sample. The dot density is $3.8 \cdot 10^{10}$ cm^{-2} with a mean height of $5.1 \pm 1nm$ and a diameter of $36 \pm 8nm$. (b) AFM image of a single quantum dot.

In order to calculate QD transition energies from the measured dot dimensions, we have implemented a simulation code based on effective mass approximation in cylindrical coordinates[13]. For this purpose we modeled the dots as truncated cones[14], with height and width as obtained from the AFM analysis. From the simulations we obtained an inter-subband absorption peak at 183 meV involving ground state and the last excited state of QD.

Fig.3 shows the energy band diagram at thermal equilibrium and room temperature of the QDIP under study. We calculated the device band diagram using a quantum-corrected transport-Poisson model[15,16]. Material parameters are taken from the literature assuming GaAs/Al$_{0.3}$Ga$_{0.7}$As CB discontinuity of 62%, as determined by C-V profiling technique[17]. The device exhibits two sharp band discontinuities due to the presence of the doped AlGaAs
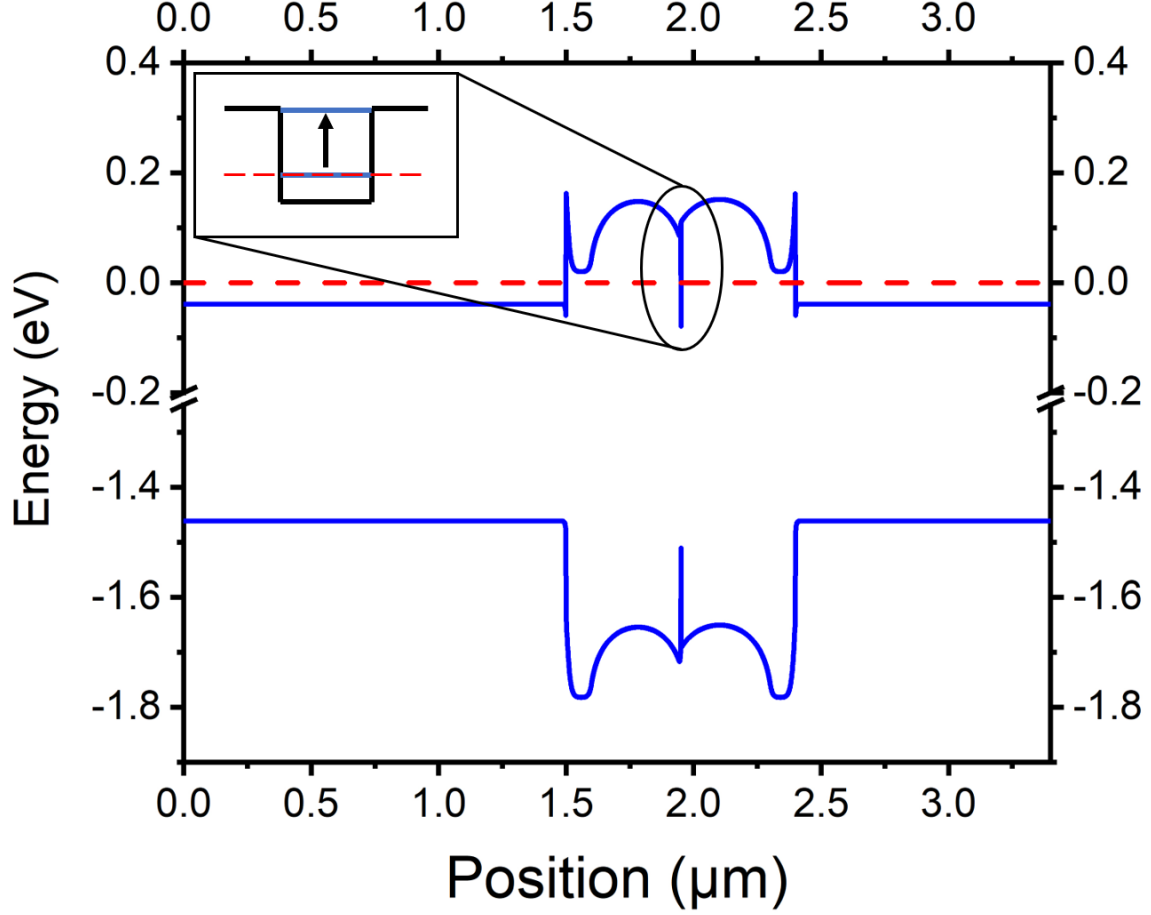
FIG. 3: Structure of the device and band alignment of the QDIP under study. The inset shows the calculated QDs ground and excited state involved in the transition.

regions which could enhance carrier injection into the semi-insulating material.

The optoelectronic characterization of the devices was performed at a temperature of 77 K by applying a bias to the top contact with respect to the sample bottom contact and measuring the resulting current. Figure 4 shows typical dark-current characteristics, obtained by blocking the cryostat windows by a cooled shield. The asymmetry of the dark-current curve is most likely related to an asymmetric charge distribution along the growth direction. The latter is probably due to the large band offset between the GaAs and AlGaAs regions in combination with the low operating temperature.
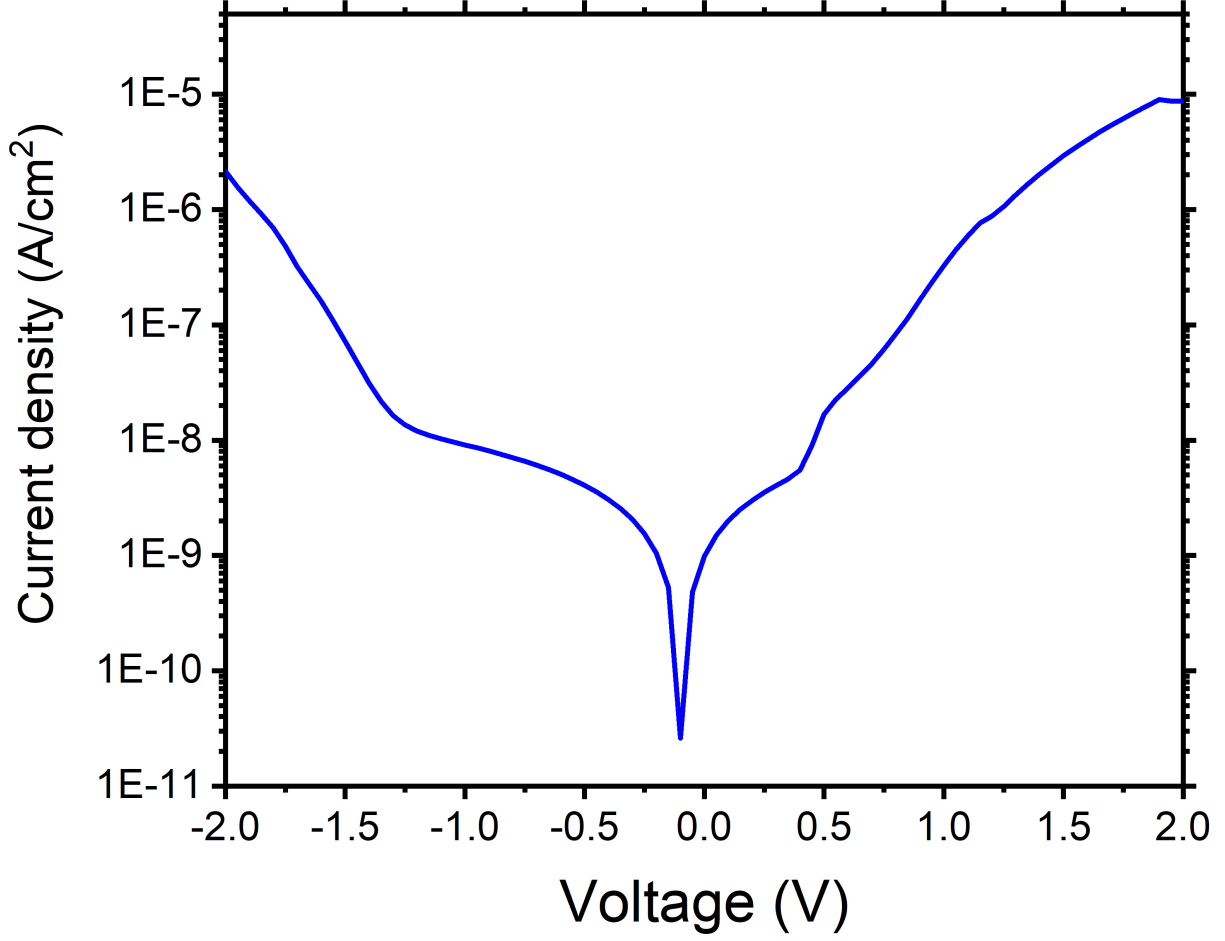
FIG. 4: Dark current density measured at 77 K from -2 V to +2 V.

Photocurrent spectra were obtained in lock-in technique by illuminating the device by the chopped globar source in a Fourier-transform infrared spectrometer (FTIR). The QDIP current response was measured by a low-noise current amplifier and employed as FTIR detector input. Figure 5 shows the photocurrent spectrum recorded at an applied bias of -2 V, featuring a narrow peak with a full width of half maximum of 23 meV centered around 198 meV. This result is in good agreement with the simulated dot transition energy at 183 meV (black arrow), clearly indicating that the photocurrent peak originates from a quantum dot intersubband transition.

This achievement demonstrates the potential of droplet epitaxy for applications where an optical intersubband transition with a precisely selectable energy and a narrow linewidth is required, thanks to the high control over dot geometrical properties. Moreover, the achieved high dot densities allows the observation of a photocurrent response based on dot intersub-
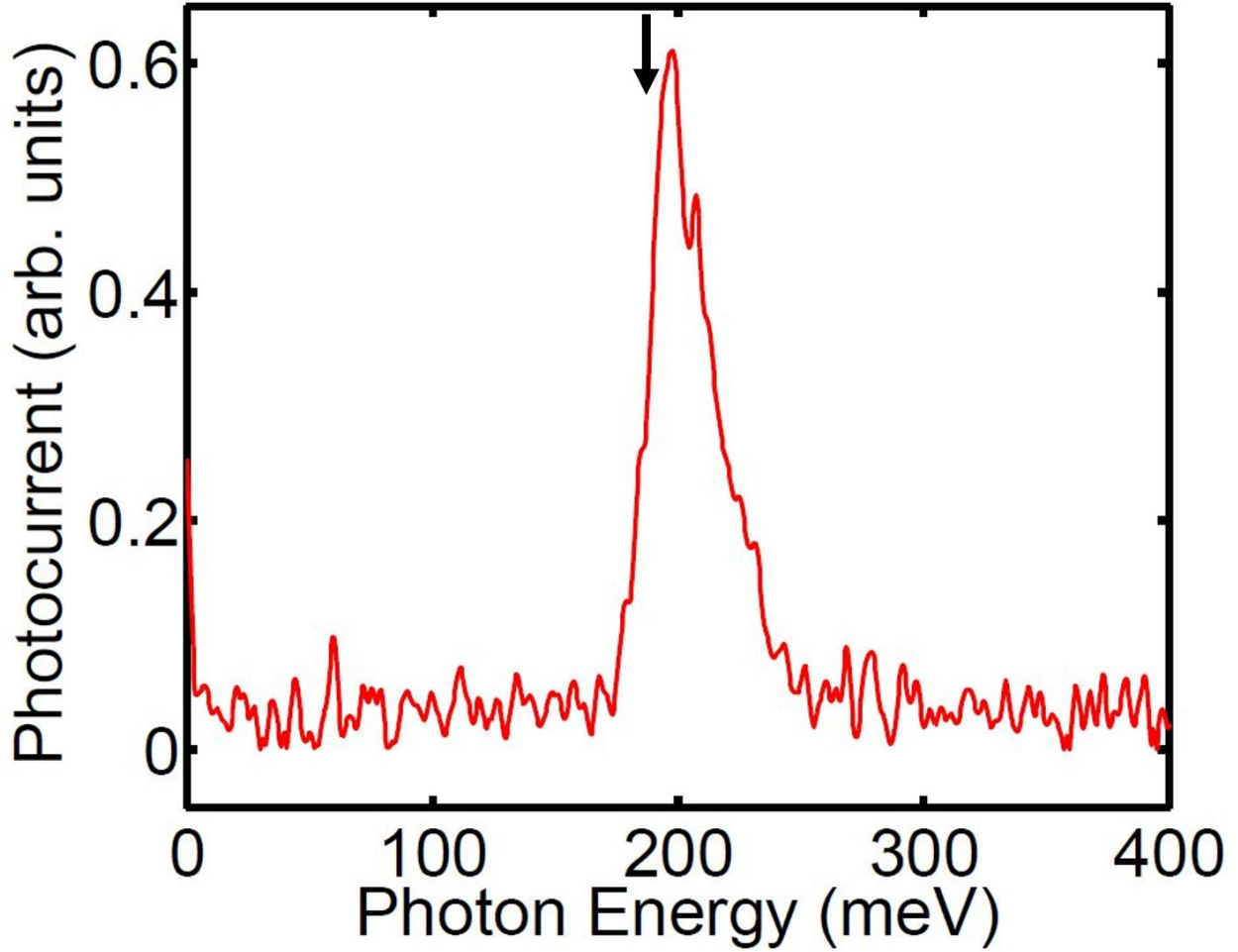
band transitions already in a single-layer device.

FIG. 5: Photocurrent spectrum measured at 77 K and a bias of -2 V. The black arrow indicates the simulated intersubband transition energy.

V. CONCLUSIONS

The higher number of independent parameters (QD geometry, dimensions and density) and the narrow size dispersion make DE-QDIP a promising alternative to SK-QDIP for IR detection, in particular when a narrow absorption band is required[18]. In this work we report the first example of a working QDIP based on DE-QDs, suitable for TIR detection. The high dot density achieved allowed us to observe a clear photocurrent signal for a single layer of QDs. The high uniformity of DE-QDs resulted in a photocurrent peak centered at 198 meV with a narrow bandwidth of 23 meV. The identification of the measured peak with a QD

transition was confirmed by simulations based on effective mass approximation. We believe that the ability to finely tune the geometrical properties of QDs make droplet epitaxy an attractive technique for QDIPs, since it can overcome most of the limiting problems of the current generation of dot-based detectors.

REFERENCES

[1] A. Rogalski, J. Antoszewski, and L. Faraone, "Third-generation infrared photodetector arrays," Journal of Applied Physics **105** (2009).

[2] C. Downs and T. E. Vandervelde, "Progress in infrared photodetectors since 2000," Sensors (Switzerland) **13**, 5054–5098 (2013).

[3] S. Bietti, A. Scaccabarozzi, C. Frigeri, M. Bollani, E. Bonera, C. V. Falub, H. Von Känel, L. Miglio, and S. Sanguinetti, "Monolithic integration of optical grade GaAs on Si (001) substrates deeply patterned at a micron scale," Applied Physics Letters **103** (2013), 10.1063/1.4857835.

[4] L. Cavigli, S. Bietti, N. Accanto, S. Minari, M. Abbarchi, G. Isella, C. Frigeri, A. Vinattieri, M. Gurioli, and S. Sanguinetti, "High temperature single photon emitter monolithically integrated on silicon," Applied Physics Letters **100** (2012), 10.1063/1.4726189.

[5] O. P. Bolkhovityanov, Yu B and Pchelyakov, "GaAs epitaxy on Si substrates: modern status of research and engineering," Uspekhi Fizicheskih Nauk **178**, 459 (2008).

[6] A. Rogalski, "Infrared detectors: An overview," Infrared Physics and Technology **43**, 187–210 (2002).

[7] P. Martyniuk and A. Rogalski, "Quantum-dot infrared photodetectors: Status and outlook," Progress in Quantum Electronics **32**, 89–120 (2008).

[8] S. Raghavan, P. Rotella, A. Stintz, B. Fuchs, S. Krishna, C. Morath, D. A. Cardimona, and S. W. Kennerly, "High-responsivity, normal-incidence long-wave infrared ($\lambda 7. 2\mu$m) InAs/In0.15Ga0.85As dots-in-a-well detector," Applied Physics Letters **81**, 1369–1371 (2002).

[9] S. F. Tang, S. Y. Lin, and S. C. Lee, "Near-room-temperature operation of an InAs/GaAs quantum-dot infrared photodetector," Applied Physics Letters **78**, 2428–2430 (2001).

[10] J. Phillips, "Evaluation of the fundamental properties of quantum dot infrared detectors," Journal of Applied Physics **91**, 4590–4594 (2002).

[11] F. B. Basset, S. Bietti, A. Tuktamyshev, S. Vichi, E. Bonera, and S. Sanguinetti, "Spectral broadening in self-assembled GaAs quantum dots with narrow size distribution," J. Appl. Phys. (accepted for pubblication).

[12] C. Somaschini, S. Bietti, A. Fedorov, N. Koguchi, and S. Sanguinetti, "Concentric Multiple Rings by Droplet Epitaxy: Fabrication and Study of the Morphological Anisotropy," Nanoscale Research Letters **5**, 1865–1867 (2010).

[13] J.-Y. Marzin and G. Bastard, "Calculation of the energy levels in quantum dots," Solid State Communications **92**, 437–442 (1994).

[14] S. Bietti, J. Bocquel, S. Adorno, T. Mano, J. G. Keizer, P. M. Koenraad, and S. Sanguinetti, "Precise shape engineering of epitaxial quantum dots by growth kinetics," Physical Review B **92**, 075425 (2015).

[15] M. Gioannini, A. P. Cedola, N. Di Santo, F. Bertazzi, and F. Cappelluti, "Simulation of quantum dot solar cells including carrier intersubband dynamics and transport," IEEE Journal of Photovoltaics **3**, 1271–1278 (2013).

[16] A. Khalili, A. Tibaldi, F. Elsehrawy, and F. Cappelluti, "Multiscale device simulation of quantum dot solar cells," Proceedings of SPIE **10913**, 59 (2019).

[17] M. O. Watanabe, J. Yoshida, M. Mashita, T. Nakanisi, and A. Hojo, "Band discontinuity for GaAs/AlGaAs heterojunction determined by C-V profiling technique," Journal of Applied Physics **57**, 5340–5344 (1985).

[18] J. A. Sobrino and J. C. Jiménez-Muñoz, "Minimum configuration of thermal infrared bands for land surface temperature and emissivity estimation in the context of potential future missions," Remote Sensing of Environment **148**, 158–167 (2014).